12-2010

Coercivity and Exchange Bias of Mn0.25Ti1.1S2 in the Cluster-Glass State

P. M. Shand
University of Northern Iowa

T. Rash
University of Northern Iowa

See next page for additional authors

Coercivity and exchange bias of $Mn_{0.25}Ti_{1.1}S_2$ in the cluster-glass state

P. M. Shand, T. Rash, M. Streicher, and T. E. Kidd
Department of Physics, University of Northern Iowa, Cedar Falls, Iowa 50614-0150, USA

K. R. Boyle and L. H. Strauss
Department of Chemistry and Biochemistry, University of Northern Iowa, Cedar Falls, Iowa 50614-0150, USA

(Received 11 June 2010; published 10 December 2010)

Magnetic measurements have been carried out on the Mn-intercalated transition-metal dichalcogenide $Mn_{0.25}Ti_{1+y}S_2$. The material, which contained a concentration $y \approx 0.1$ of excess intercalated Ti, exhibited paramagnetic behavior at high temperatures with an effective moment per Mn ion of $\mu_{eff}=6.07\pm0.23\ \mu_B$, which shows that the system comprises localized Mn^{2+} moments. A Curie-Weiss temperature $\Theta_{CW}=-26\pm1$ K indicated that antiferromagnetic interactions were dominant. Deviation from Curie-Weiss behavior below 100 K signaled the formation of antiferromagnetically correlated clusters. Bifurcation of the zero-field-cooled and field-cooled magnetizations below 20 K indicated a transition to a cluster-glass state. The cluster-glass state exhibited hysteresis and a loop shift indicating exchange bias. The behavior of the coercivity and exchange bias can be understood using a model in which frozen spins at the periphery of a cluster interact with the antiferromagnetically correlated interior.

DOI: 10.1103/PhysRevB.82.214413 PACS number(s): 75.50.Lk, 75.60.Ej

I. INTRODUCTION

Transition-metal dichalcogenides possess a layered crystal structure in which intralayer bonds between the transition-metal atoms (M) and the chalcogen atoms (Ch) are strong but interlayer coupling from van der Waals interactions is relatively weak. These MCh_2 compounds can serve as hosts for foreign atoms, which are incorporated in the van der Waals gaps between the layers to form an intercalated system. A large number of such intercalated systems have been studied because they exhibit a rich variety of electronic and magnetic properties.[1,2] For example, pure $TiSe_2$ exhibits an unusual charge-density-wave (CDW) ground state, the origin of which has been hotly debated for many years.[3–6] It was recently discovered that the introduction of Cu as an intercalant in $TiSe_2$ leads, at a high enough doping level, to a superconducting ground state that competes with the CDW phase.[7–10]

Titanium dichalcogenides intercalated with magnetic atoms are an enticing system for the investigation of the effects of itinerant carriers, disorder, and low dimensions on magnetism. For example, Fe_xTiS_2 (where Fe is the intercalant) exhibits a succession of transitions at low temperatures from ferromagnetism (FM) to re-entrant ferromagnetism to spin glass (SG) as the concentration x is decreased.[11,12] This behavior is reminiscent of canonical three-dimensional spin glasses such as $Au_{1-x}Fe_x$.[13,14] This resemblance is not accidental. In both types of materials, the Ruderman-Kittel-Kasuya-Yosida (RKKY) interaction is responsible for the exchange coupling between the localized moments.[14,15] In spin-glass materials such as $Au_{1-x}Fe_x$ and $Cu_{1-x}Mn_x$, at low x (<5 at. %), the spin-glass state is favored because of the random positioning of the substituted ions and the frustration induced by the oscillatory RKKY coupling. A greater concentration of substituents brings about ordering at short length scales (e.g., nearest and next-neighbor distances) and if the concentration of carriers is high enough, the RKKY interaction will favor long-range ferromagnetic ordering. In some cases, e.g., $Au_{1-x}Fe_x$, there is a *re-entrant* transition at low temperatures where the long-range ordered ferromagnetic state (that contains, however, substantial disorder) gives way to a cluster-glass (CG) state characterized by correlated regions of large but finite size.[14]

In this paper, we examine the magnetic properties of $Mn_xTi_{1+y}S_2$ with $x=0.25$ and $y \approx 0.1$. The concentration y represents excess Ti intercalated in the TiS_2 system along with Mn. The excess Ti, which typically attends the crystal-growth process,[16] plays an important role in determining the magnetic behavior of the Mn ions as we argue below. Thus, we explicitly indicate the excess Ti in the chemical formula of the sample. Previous work[17] has shown that $Mn_{0.2}TiS_2$ (with some excess Ti probably present) exhibits paramagnetic behavior for temperatures $T>15$ K. Below 15 K, the field-cooled (FC) and zero-field-cooled (ZFC) magnetizations no longer overlapped, which indicated the existence of a spin-glasslike state at low temperatures. As in Fe_xTiS_2, the spin-glasslike behavior is likely driven by the RKKY interaction, which should be relatively strong due to the presence of a large number of itinerant carriers.[2] The purpose of this work is to investigate the properties of this low-temperature state in $Mn_{0.25}Ti_{1+y}S_2$. The spin-glass material $Cu_{1-x}Mn_x$ at high Mn concentrations ($x>5\%$) exhibits intriguing characteristics such as hysteresis and loop shifts indicative of exchange anisotropy at low temperatures.[18,19] By comparing these characteristics with those of $Mn_{0.25}Ti_{1+y}S_2$, we hope to shed light on the mechanism for these phenomena in disordered magnetic systems.

II. EXPERIMENTAL DETAILS

Mn-intercalated TiS_2 samples were grown in a two-step process by the vapor-transport method using iodine as a carrier agent. In the first step, TiS_2 powder was synthesized using pure powders of Ti and S placed in a fused silica ampoule. The ampoule was sealed under vacuum and heated

to 750 °C for 3 days. The resulting submillimeter-diameter TiS_2 crystals were then thoroughly mixed with Mn powder and placed in a second ampoule and heated under a 700–800 °C thermal gradient for 2 weeks. The final product was a mixture of Mn-intercalated TiS_2 crystals with diameters ranging from 50 μm to several millimeters. Roughly half of the Mn was incorporated into the crystals, with the remainder forming a thin metallic film on the side of the ampoule.

After growth, the samples were examined with powder x-ray diffraction (PXRD) using a Rigaku Miniflex II system and energy dispersive x-ray spectroscopy (EDS) using a Bruker Quantax 200 spectrometer mounted on a Tescan Vega II scanning electron microscope. The PXRD measurements were taken on finely ground powder that had been passed through a 200-mesh (75 μm) sieve. The measurements showed the samples were single phase with a *c*-axis expansion consistent with a 25% Mn intercalation level.[20] No signs of superstructure associated with structural ordering of the Mn ions were seen. The EDS measurements were taken on three or more larger single-crystal samples with clean surfaces prepared by exfoliation in air just before the sample was inserted into the microscope. Several readings were taken over the surface of each sample that was investigated. These measurements showed that the samples were homogenous with formula unit $Mn_xTi_{1+y}S_2$, with $x=0.25\pm0.02$ and $y=0.1\pm0.05$. The rather large error in the excess Ti concentration reflects mostly variations between sample crystals used in the EDS measurements, suggesting local surface effects (e.g., due to oxidation). As mentioned before, excess Ti is a common issue in the synthesis of TiS_2 crystals.[16] The extra Ti ions are located at intercalation sites with +4 and +3 oxidation states.[21]

The $Mn_{0.25}Ti_{1.1}S_2$ sample used in our investigations consisted of a large number of small single crystals compacted in a cylindrical form to give a mass of 89 mg. dc magnetization measurements on the sample were performed with a Quantum Design physical property measurement system (PPMS) with the ac/dc magnetization option. The magnetic field was applied along the axis of the cylindrical sample. We also did measurements with the field perpendicular to the cylindrical axis to check for orientation effects. There were slight (<5%) differences in the magnitude of the magnetization at a given field but no qualitative differences in behavior. In performing all the measurements, we were careful to allow enough time for thermal equilibration of the sample and sample chamber to avoid spurious temperature-dependent hysteretic effects. When the sample was in "zero field," i.e., no current in the superconducting magnet, the actual field experienced by the sample was the sum of the Earth's field and the remanent field of the magnet (<10 Oe). Field cooling was done by cooling the sample in various applied fields from 100 K down to the measurement temperature. After the completion of a hysteresis-loop measurement at this temperature, the applied field was oscillated to zero and the sample warmed to 100 K. The sample was kept at 100 K for at least 10 min before setting the field for the next field-cooling process.

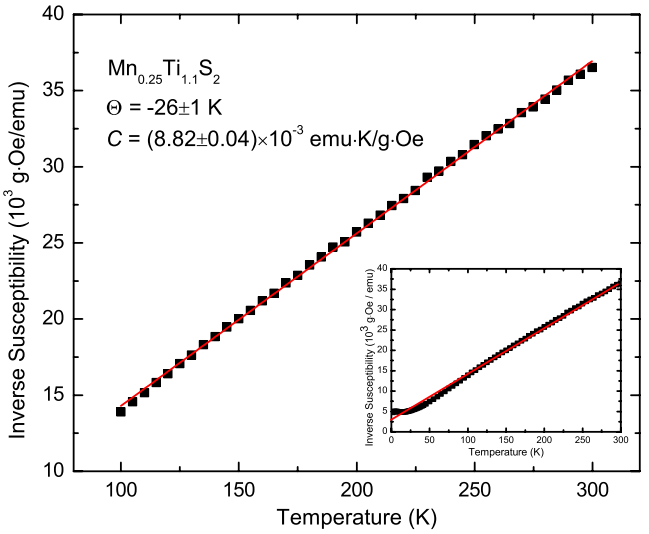

FIG. 1. (Color online) Inverse susceptibility $(1/\chi)$ versus temperature (T) for 100 K$\leq T\leq$300 K. The measuring field was 1 kOe. The solid line is a fit to the Curie-Weiss law. The inset shows the $1/\chi$ data for temperatures down to 2 K. The data deviate from the Curie-Weiss fit at ~100 K.

III. RESULTS

Measurement of the susceptibility $\chi(=M/H)$ of the Mn ions in $Mn_{0.25}Ti_{1.1}S_2$ for temperatures in the range 2 K$\leq T\leq$300 K indicated paramagnetic behavior for $T>100$ K. Figure 1 shows a plot of inverse susceptibility versus temperature for 100 K$\leq T\leq$300 K along with a fit to the Curie-Weiss law $\chi^{-1}=(T-\Theta_{CW})/C$, where $C=N\mu_B^2g^2S(S+1)/3k_B$ is the Curie constant and Θ_{CW} is the Curie-Weiss temperature. It should be noted that the susceptibility data displayed in Fig. 1 were obtained by subtracting the contribution of TiS_2 to the total susceptibility of the sample. The susceptibility of TiS_2 was obtained by measuring a TiS_2 sample grown under similar conditions as the $Mn_{0.25}Ti_{1.1}S_2$ sample. The Curie-Weiss fit to the data is very good, with best-fit values of $C=(8.82\pm0.04)\times10^{-3}$ emu K/g Oe and $\Theta_{CW}=-26\pm1$ K. Using the value $x=0.25\pm0.02$ obtained from EDS and PXRD, and taking the concentration of excess intercalated Ti to be 0.1 ($\pm$0.05), we obtain an effective moment value $\mu_{eff}=\sqrt{g^2S(S+1)}=6.07\pm0.23$ μ_B for a single Mn ion, in agreement with previous work on Mn_xTiS_2.[17] This value of μ_{eff} value is consistent with the value 5.92 μ_B for an isolated Mn^{2+} ion, indicating that the magnetic behavior of the system is due to local Mn^{2+} moments. Though our experimental μ_{eff} value agrees with the local-moment value for Mn^{2+}, it is possible that our experimental quantity is a bit higher because of polarization effects due to the intercalated Ti ions.

The inset of Fig. 1 shows the data for the entire temperature range of the measurements. The solid line is the fit described above. Clearly, below ~100 K, the data fall below the fit line; in other words, the slope of the χ^{-1} versus T graph increases. If we define the effective moment of a Mn spin[14] as

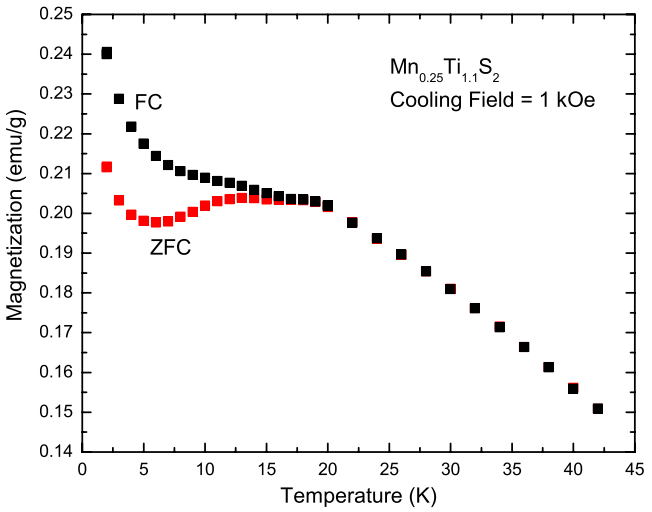

FIG. 2. (Color online) ZFC magnetization and FC magnetization as functions of temperature. For the FC measurement, a field of 1 kOe was applied at 100 K and the sample was cooled to 2 K in this field.

$$p(T) = \left[\frac{N\mu_B^2}{3k_B}\frac{d(\chi^{-1})}{dT}\right]^{-1/2}, \tag{1}$$

it is clear that p decreases for $T < 100$ K. This indicates that antiferromagnetically (AF) correlated regions, or clusters, are beginning to form. Note that the low-temperature deviation from the Curie-Weiss law is modest, which suggests the presence of competing FM interactions.

In Fig. 2, the ZFC magnetization and FC magnetization are plotted as functions of temperature. For the FC measurement, a cooling field $H_{cool}=1$ kOe was used. The field cooling was initiated at 100 K. We see that $M_{\mathrm{ZFC}}(T)$ and $M_{\mathrm{FC}}(T)$ separate below $T \approx 20$ K. The difference $M_{\mathrm{FC}}-M_{\mathrm{ZFC}}$, which is a measure of the thermoremanent magnetization, increases as the temperature decreases. There is a weak peak in $M_{\mathrm{ZFC}}(T)$ at $T_p \approx 12$ K. The irreversibility in the magnetization for temperatures below a temperature T_{irr} is a characteristic of disordered systems such as SGs and CGs. In view of the relatively large concentration of Mn, the absence of a strong peak at T_{irr}, and the fact that T_{irr} is greater than the temperature at which $M_{\mathrm{ZFC}}(T)$ peaks, we attribute the magnetic irreversibility in $Mn_{0.25}Ti_{1.1}S_2$ to CG behavior. The negative sign of Θ_{CW} indicates that the nearest-neighbor exchange interaction between Mn ions within the clusters is AF. Interestingly, M_{ZFC} goes through a minimum at ~5 K and then increases at lower temperatures, which seems unusual; $M_{\mathrm{ZFC}}(T)$ typically decreases monotonically with decreasing temperature below T_{irr}, in disordered systems. However, an increase in $M_{\mathrm{ZFC}}(T)$ for $T < T_{irr}$ has been observed in CG systems,[22,23] FM nanoparticles,[24] and disordered ferromagnets.[25–27] We also note that the upturn is not likely to be due to paramagnetic impurities because the upturn becomes a *downturn* when large enough measuring fields (>25 kOe) are used.

To further investigate the nature of the low-temperature magnetic state, T_{irr} was determined for various values of applied field H ($H=H_{cool}$). The graph of T_{irr} versus H is shown in Fig. 3. The mean-field theory of vector spin glasses with random anisotropy[28] predicts temperature-field phase-transition lines that can be described by the power-law expression[29]

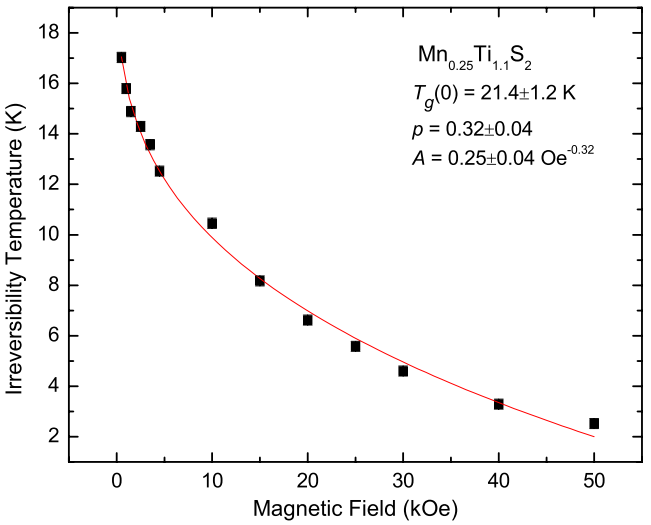

FIG. 3. (Color online) Irreversibility temperature (T_{irr}) versus magnetic field applied during field cooling. T_{irr} is the temperature at which the ZFC and FC magnetization plots bifurcate. The error in each value of T_{irr} is about the same as the height of the marker. The solid line represents a fit to Eq. (2) in the text.

$$T_g(H) = T_g(0)[1 - AH^p], \tag{2}$$

where $T_g(0)$ is the transition temperature in zero applied field and A is a parameter that depends on the strength of the anisotropy, the variance of the random exchange, and the number of components of a spin. The anisotropy is assumed to be weak relative to the exchange. The value of the exponent p depends on the strength of the anisotropy relative to the field. In the strong anisotropy (strong irreversibility) regime, one finds $p=\frac{2}{3}$, which corresponds to the de Almeida-Thouless (AT) line for Ising spins.[30] In the weak anisotropy (weak irreversibility) regime, $p=2$, which defines the Gabay-Toulouse (GT) line.[31] Using T_{irr} as a measure of the transition temperature T_g,[29,32] we fitted our data using Eq. (2). The best-fit values were $T_g(0)=21.4\pm1.2$ K, $p=0.32\pm0.04$, and $A=0.25\pm0.04$ $\mathrm{Oe}^{-0.32}$. Clearly, our $Mn_{0.25}Ti_{1.1}S_2$ system does not display either AT or GT behavior in the H-T space that we investigated.

Kotliar and Sompolinsky[33] (KS) parametrized the problem theoretically in terms of the dimensionless variables $h=\mu H/k_BT$ and $d=D/k_BT$, where μ is the magnetic moment of a spin and D is the strength of the random Dzyaloshinskii-Moriya (DM) anisotropy. Both h and d are assumed to be small. KS found that for $d \gg h^{2/3}$ (strong anisotropy regime), the exponent p describing the shape of the T_{irr}-H line is equal to $\frac{2}{3}$, i.e., AT-type behavior is recovered. For $d \ll h^{5/2}$ (weak anisotropy regime), GT-type characteristics ensue. However, if $h^{5/2} \ll d \ll h$ (intermediate anisotropy regime), KS obtained $p=\frac{1}{3}$, which is consistent with our best-fit value. For our data, $h<1$ for field strengths smaller than ~20 kOe.

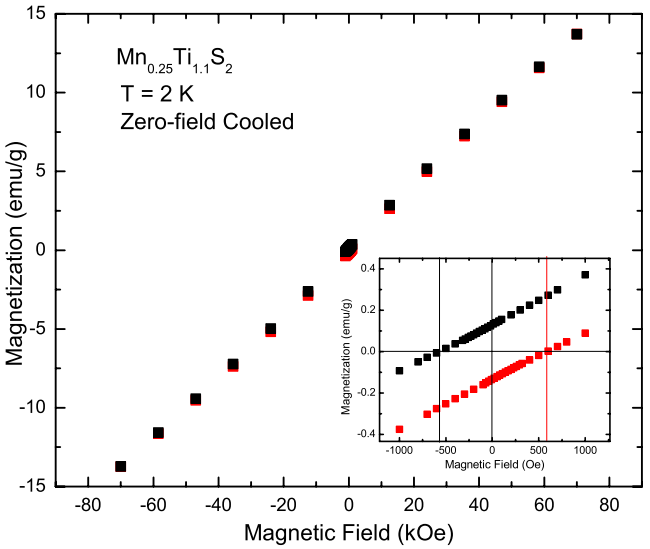

FIG. 4. (Color online) Zero-field-cooled hysteresis-loop data at $T=2$ K. The inset shows an expanded view of the data near the origin. The loop is symmetric in this case.

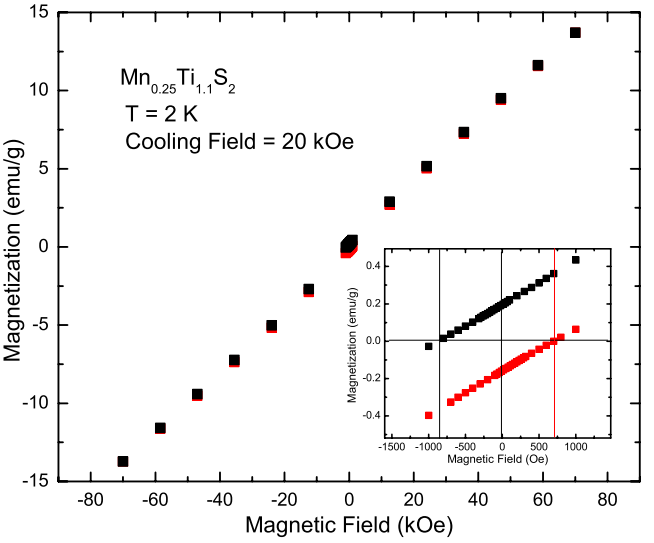

FIG. 5. (Color online) Field-cooled hysteresis-loop data at $T=2$ K. The sample was cooled from 100 K in a field of 20 kOe. The inset shows an expanded view of the data near the origin. The loop is shifted in the direction of negative fields.

These results suggest that there is significant, but not strong, random anisotropy in the $Mn_{0.25}Ti_{1.1}S_2$ system. This is supported by the fact that the difference $M_{FC}-M_{ZFC}$ remains modest down to the lowest measurement temperatures.[34]

In Fig. 4, we present hysteresis data taken at $T=2$ K. The sample was cooled in zero field down to the measurement temperature. The maximum field magnitude during the cycle was 70 kOe; on this scale, the hysteresis-loop width is rather small. The magnetization varies linearly with the field at high fields with no hint of saturation at 70 kOe. Disordered systems such as SGs and CGs are typically very difficult to saturate because of frustration or random anisotropy. A high-field susceptibility can be generated by a relatively small number of "loose" spins that are weakly coupled to spins that are bound in short-range-ordered or long-range-ordered clusters. However, in our case, the slope of the linear portion of the M versus H graph (i.e., the high-field susceptibility) is only slightly less than the low-field susceptibility (both dc and ac) at T_{irr}. In fact, the value of the slope is virtually constant for temperatures between T_{irr} and the base temperature of our measurements (2 K) as will be shown later in this section. It follows that the behavior at high fields is due to the "background" of antiferromagnetically correlated clusters, which constitutes the large majority of the spin system. The hysteresis that is superimposed on this background results from dissipation as the spin system is field cycled. The inset shows the data in the vicinity of the origin more clearly. The upper and lower branches cross $M=0$ at field values of equal magnitude; thus, the hysteresis loop is symmetric.

To explore the effect of field cooling on the hysteresis loop, the $Mn_{0.25}Ti_{1.1}S_2$ sample was cooled from 100 to 2 K in a 20 kOe field. The resulting data are shown in Fig. 5. There is no difference in the high-field behavior upon field cooling. The high-field magnetization is completely reversible at all temperatures and field cooling has no effect on this behavior. However, the inset shows that the hysteretic response is affected by field cooling; the loop is displaced along the field axis, one of the hallmarks of exchange bias. Cooling from 300 K instead of 100 K in the same 20 kOe field produced no significant change in the hysteresis loop.

To investigate the hysteresis loop in a more quantitative fashion, we fitted the low-temperature $M(H)$ data to an expression consisting of two terms: (i) a linear term representing the dominant reversible response of the AF clusters and (ii) a phenomenological hysteretic term that captures the coercivity and exchange-bias effects. The expression is[26,35]

$$M(H) = \chi_{AF}H + M_0\left(\frac{2}{\pi}\right)\tan^{-1}\left[\left(\frac{H \pm H_c}{H_c}\right)\tan\left(\frac{\pi S}{2}\right)\right]. \tag{3}$$

In Eq. (3), χ_{AF} is the background susceptibility, H_c is the coercivity, M_0 is the saturation magnetization of the hysteretic component, and S is a squareness parameter that describes the shape of the hysteresis loop ($0<S<1$). Note that the upper and lower branches of the loop were fitted separately. Figure 6 shows the same data presented in Fig. 5 along with the fit using Eq. (3). The fit is excellent over the entire range of field values. The upper inset shows the two components of the fit separated. For clarity, only the upper branch of the hysteretic component is shown. Its shape indicates that the magnetization of the hysteretic component is changing little with increasing field at 70 kOe. The lower inset shows the data and fit in the low-field region. Fits were also carried out for hysteresis data obtained using different cooling fields.

The values of the best-fit parameters for each value of H_{cool} are presented in Table I. The temperature was 2 K in every case. There were slight differences between the values of M_0 and S for the upper and lower branches of the loop; these values were averaged. The coercivity of the system was calculated as $H_c=(H_c^{lwr}-H_c^{upr})/2$ and the presumed exchange-bias field was obtained from $H_{EB}=(H_c^{lwr}+H_c^{upr})/2$.

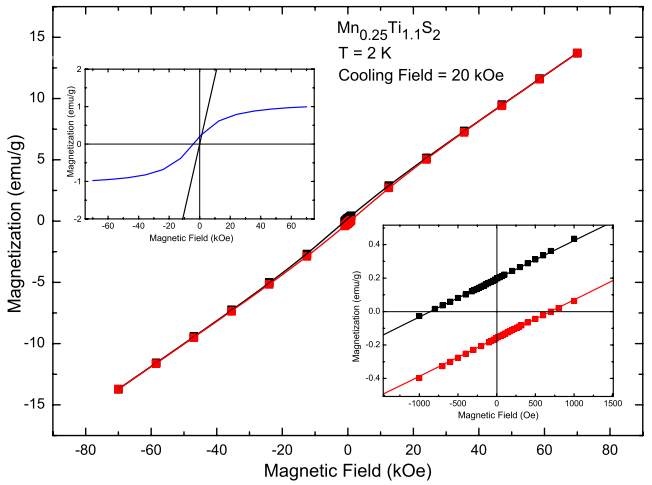

FIG. 6. (Color online) Field-cooled hysteresis-loop data at $T=2$ K fitted (bold lines) according to Eq. (3) in the text. The upper inset shows the variation in the two separate terms of the fitting function for the upper branch of the hysteresis loop. The lower inset presents an expanded view of the data and fit in the vicinity of the origin.

The following general trends are apparent from the data. (i) The bias field is negative, which is to say, opposite to the direction of the cooling field, for 20 kOe$\leq|H_{cool}|\leq$50 kOe. (50 kOe is the highest cooling field used in our measurements.) (ii) The ZFC coercivity is smaller than the FC coercivities. (iii) $|H_{EB}|$ decreases with increasing $|H_{cool}|$ for $|H_{cool}|>20$ kOe (which is the lowest cooling field used in our measurements). (iv) The ZFC value of the parameter M_0 is greater than the FC values. The FC value of M_0 increases with $|H_{cool}|$ for 20 kOe$\leq|H_{cool}|\leq$50 kOe. (v) The ZFC value of the parameter S is smaller than the FC values, i.e., the loop becomes more square as a result of field cooling. (vi) The linear contribution to $M(H)$ is essentially independent of $|H_{cool}|$ as indicated by the constant value of χ_{AF}. It is useful to note that the results for $H_{cool}=-40$ kOe are consistent with the trends suggested by the results for positive values of H_{cool}, which indicates that the exchange-bias effect is robust and largely independent of the direction of the cooling field.

Table II shows the dependence of the ZFC coercivity on temperature. There is a monotonic decrease in H_c^{ZFC} with temperature, becoming negligible in the vicinity of 15 K. Recalling that the zero-field irreversibility temperature $T_{irr}(0)\equiv T_g(0)=21.4$ K, it is clear that the hysteretic behavior is associated with the CG phase below T_{irr}. Finally, we note that the H_c^{ZFC} values of 3.06 kOe at 2 K and 2.23 kOe at 5 K are greater than one might expect for a system of spin-only Mn^{2+} ions. For example, in $Cu_{1-x}Mn_x$, H_c^{ZFC} values are <100 Oe.[14,18,19] In Mn-based FM semiconductors such as $Ga_{1-x}Mn_xAs$, H_c^{ZFC} is typically <200 Oe.[36]

IV. DISCUSSION

A. Cluster-glass state

The microscopic interactions and structure of $Mn_{0.25}Ti_{1.1}S_2$ endow it with characteristics common to both canonical SGs such as $Cu_{1-x}Mn_x$ and disordered, geometrically frustrated magnetic materials. The latter materials include, for example, II-VI-based diluted magnetic semiconductors (DMSs) (Ref. 37) and disordered geometrically frustrated antiferromagnets (GFAs).[38,39] In canonical metallic SGs, the freezing transition is driven by disorder and frustration in the exchange coupling due to the oscillating RKKY interaction. The spin-glass behavior observed in both II-VI DMSs and GFAs is due to purely geometric frustration in the presence of disorder. In $Mn_{0.25}Ti_{1.1}S_2$, however, the Mn^{2+} ions experience both geometric frustration (due to the hexagonally ordered nets formed by the Mn intercalants) and exchange frustration arising from the RKKY interaction. Further, in II-VI DMSs and disordered GFAs, the ratio $|\Theta_{CW}|/T_f$ (where T_f is the freezing temperature) is relatively large. For example, in $SrCr_8Ga_4O_{19}$, which is a GFA with a Kagomé lattice, $|\Theta_{CW}|/T_f=125$.[40] In contrast, $|\Theta_{CW}|/T_f\approx 1$ for $Mn_{0.25}TiS_2$. [We take $T_f=T_g(0)$, i.e., the zero-field irreversibility temperature.] The small value of the $|\Theta_{CW}|/T_f$ ratio arises from the fact that there are further-neighbor FM interactions (due to RKKY exchange) that partially offset the nearest-neighbor AF interactions. It should be noted that $x=0.25$ is the concentration corresponding to a $2a\times 2a$ in-plane superlattice formation by the Mn intercalants. However, local departures from $x=0.25$ and the presence of excess Ti will likely result in only short-range positional ordering of the Mn ions, with groups of Mn ions being forced to smaller separation distances because of the highly charged Ti^{3+} or Ti^{4+} ions. This scenario is in agreement with Monte Carlo studies that we have done.[41] This short-range spatial order, along with frustration of magnetic interactions, drives the observed transition to a cluster-glass state. We note that other workers[12,42] have found paramagnetic behavior in

TABLE I. Fitting parameters obtained when Eq. (3) in the text is used to describe the field-cooled hysteresis-loop data. Note that the 40 kOe cooling field was applied in the opposite direction to the other cooling fields.

H_{cool} (kOe)	T (K)	M_0 (emu/g)	H_c^{upr} (kOe)	H_c^{lwr} (kOe)	H_c (kOe)	S	H_{EB} (kOe)	χ_{AF} (emu/g Oe)
0	2	1.73	3.04	3.07	3.06	0.078	0	1.8×10^{-4}
20	2	1.17	4.03	3.27	3.65	0.15	−0.38	1.8×10^{-4}
−40	2	1.33	3.15	3.58	3.36	0.13	0.21	1.8×10^{-4}
50	2	1.50	3.78	3.43	3.61	0.11	−0.18	1.8×10^{-4}

TABLE II. Zero-field-cooled coercivity (obtained from fits to the hysteresis data) versus temperature.

T (K)	H_c^{ZFC} (kOe)
2	3.06
5	2.23
10	0.71
15	0.005

Mn_xTiS_2 for $x<0.33$ and for temperatures down to 5 K. This is due to either smaller amounts of excess intercalated Ti in their samples or an actual Mn concentration smaller than the nominal value.

Based on our comments above, one would expect that a SG material such as $Cu_{1-x}Mn_x$ with a high concentration of Mn should bear some similarity in magnetic behavior to $Mn_{0.25}Ti_{1.1}S_2$. Kouvel[18,19] has carried out extensive investigations on $Cu_{1-x}Mn_x$ and $Ag_{1-x}Mn_x$ with x between 0.05 and 0.3. The magnetic behavior for both high- and low-temperature regimes was indeed similar to what we have observed in $Mn_{0.25}TiS_2$. For example, in $Cu_{1-x}Mn_x$ and $Ag_{1-x}Mn_x$, there was Curie-Weiss behavior with negative Θ_{CW} at high temperatures, with a change in slope in the $1/\chi$ versus T graph at lower temperatures. In addition, hysteresis and exchange-biaslike effects were observed at low temperatures. Further, the low-temperature magnetization could be modeled as the sum of one component linear in the field and a second component that gave rise to hysteresis. There were also some notable differences: (i) in $Cu_{1-x}Mn_x$ and $Ag_{1-x}Mn_x$, the coercivity was smaller in magnitude than the exchange-bias field at the lowest temperatures. The opposite is true for $Mn_{0.25}Ti_{1.1}S_2$. (ii) In $Cu_{1-x}Mn_x$ and $Ag_{1-x}Mn_x$, at the lowest temperatures, the magnetization of the hysteretic component was comparable to that of the linear component at the highest fields. However, the linear contribution is dominant at high fields in $Mn_{0.25}Ti_{1.1}S_2$. To qualitatively explain the behavior of $Cu_{1-x}Mn_x$ and $Ag_{1-x}Mn_x$, Kouvel posited that statistical fluctuations in the distribution of Mn ions lead to antiferromagnetically correlated clusters with net moments that are generally not zero. Field cooling aligns these net moments, which remain partially aligned when the field is removed due to local anisotropy. A similar model was used to explain exchange bias in granular layers of AF CoO.[43] We will make use of Kouvel's AF cluster model in addition to the domain state model[44] to explain the coercivity and exchange-bias effects observed in $Mn_{0.25}Ti_{1.1}S_2$.

B. Remanent magnetization and exchange bias

In the domain state model, disorder (e.g., due to substitution or defects) leads to the formation of domains in an antiferromagnet or a large enough AF cluster. Due to the disorder, there are uncompensated spins that can be aligned by an applied field and the resulting magnetization becomes frozen in on cooling to a temperature below T_f. Domain walls pass preferentially through nonmagnetic sites to minimize exchange energy. Rough domain walls may also themselves develop a net magnetization during field cooling. The field-cooling results in a metastable state with a remanent magnetization that decays slowly with time after the cooling field is removed. The metastability is due to pinning of the domain walls by nonmagnetic atoms and by the interaction between the domain and domain-wall magnetizations. Of course, cluster-cluster interactions also give rise to metastability because of random anisotropy and RKKY-induced frustration. The remanent magnetization produced by field cooling gives rise to the irreversible part of $M(H)$. The unidirectional anisotropy that underlies exchange bias is due to a relatively small fraction of the remanent magnetization that remains pinned in the direction of H_{cool} when the applied field is reversed and increased in magnitude.

In our model describing the low-temperature magnetic behavior of the $Mn_{0.25}Ti_{1.1}S_2$ cluster-glass system, we assume that the fraction of the remanent magnetization that rotates during hysteresis ($\vec{M}_{free}$) interacts antiferromagnetically with the pinned fraction ($\vec{M}_{pin}$). Further, $\vec{M}_{free}$ is due to uncompensated spins at the surface of each cluster. Some AF domains (weakly pinned) also contribute to this magnetization. The pinned fraction of the remanent magnetization comprises the "interface" between the AF background in the interior of the clusters and the uncompensated spins at the boundaries. The pinned interface spins give rise to the exchange bias. Domains with strongly pinned walls will also contribute to $\vec{M}_{pin}$. Our model is analogous to an "inverted" core-shell structure in which the FM shell interacts antiferromagnetically with the spins at the interface of the AF core.[45,46]

On the basis of our model, the AF interaction between the "free" fraction (aligned with H_{cool}) and the pinned fraction after field cooling will cause the high-field magnetization (M_0 in our fits) to be reduced relative to the ZFC case (in which there is negligible remanent magnetization after cooling), as we observed. The AF interaction between $\vec{M}_{free}$ and $\vec{M}_{pin}$ also explains the decrease in $|H_{EB}|$ with increasing $|H_{cool}|$ seen in our measurements. For $|H_{cool}|$ greater than some critical value, further increase in the cooling field strength will increase the parallelism of $\vec{M}_{free}$ and $\vec{M}_{pin}$. This reduces the effective unidirectional anisotropy field in the direction of $\vec{H}_{cool}$ and therefore $|H_{EB}|$ decreases. The increase in magnitude of the total remanent magnetization with increasing $|H_{cool}|$ should also increase M_0. This is indeed the trend that we observed.

We note that exchange bias has been observed in many inhomogeneous materials without well-defined interfaces between the two magnetic phases.[47] One example is the cluster-glass manganite material $LaMn_{0.7}Fe_{0.3}O_3$.[48] The effect has also been observed in other phase-separated manganites such as $Pr_{1/3}Ca_{2/3}MnO_3$.[49] In these manganite materials, the exchange-bias effect has been attributed to FM clusters embedded in SG-like host[48] or in an AF background.[49] The relatively small ratio of exchange-bias field to coercivity that we have observed in $Mn_{0.25}Ti_{1.1}S_2$ is likely due to the fact that the hysteretic phase is not an ordered ferromagnet; rather, it is a disordered, glassy phase and consequently a large unidirectional anisotropy (relative to the coercivity) is more difficult to induce. The absolute value of the exchange-

bias field is, however, quite significant and is greater than that in many other systems. We also note that the hysteresis-loop shift that we have observed is not due to the traversal of minor loops.[50] The upper inset in Fig. 6 shows that the magnetization of the hysteretic component is changing little with increasing field strength at ± 70 kOe, indicating that the subsystem is traversing a major loop.

C. Hysteresis and coercivity

To understand the nature of hysteresis and coercivity in $Mn_{0.25}Ti_{1.1}S_2$, it is instructive to examine theoretical considerations of hysteresis in the Sherrington-Kirkpatrick SG model[51,52] and the random-field Ising model (RFIM).[53] The effective local field at the position of each spin comprises contributions from isotropic exchange (RKKY and to a lesser extent superexchange), anisotropic exchange (Dzyaloshinskii-Moriya), uniaxial anisotropy (e.g., magnetocrystalline, strain), and the applied magnetic field. Because of the disorder, the direction of the anisotropy axis will vary with position. The observed hysteresis is due to irreversible spin flips that occur when the spin at a site becomes unstable in its local field. A spin flip will typically cause other spins to become unstable and flip, creating an avalanche that ceases only when a new global metastable state consistent with the local-field values is achieved. The coercivity is the field H_c for which there is a metastable state with magnetization $M(|H_c|)=0$. The value of H_c will clearly depend on the energy landscape of the spin system. In systems in which the frustration and/or random anisotropy is relatively strong, spin flips will trigger only small avalanches—the energy minima are deep and plentiful. Changing the applied field H will cause only small changes in the magnetization; therefore, the hysteresis loop is more S shaped ($S \rightarrow 0$). If there is significant FM exchange (or coherent anisotropy) tending to cause alignment along the direction of H, spin flips will cause larger avalanches, leading to a more switchinglike behavior during the hysteresis cycle, i.e., the loop becomes more square ($S \rightarrow 1$). The remanent magnetization caused by H_{cool} gives rise to an effective field akin to an exchange (or coherent anisotropy) field and thus an increase in loop squareness should be expected upon field cooling, which we indeed observed.

In most layered (and core-shell) systems that exhibit exchange bias, the FC coercivity (H_c^{FC}) is greater than the ZFC coercivity (H_c^{ZFC}). The reason is that when the FM layer rotates under the influence of a reverse field, it "drags" some of the AF boundary spins (aligned by field cooling) along with it due to the exchange coupling. The torque necessary to rotate these spins against the AF anisotropy field increases the coercivity. A similar explanation is obtained using our model for the magnetic behavior of $Mn_{0.25}Ti_{1.1}S_2$: when the free fraction rotates, it drags some of the spins of the pinned fraction with it, thereby increasing the coercivity. It is also instructive to see that an increase in H_c under field cooling is consistent with the hysteretic behavior of the RFIM. As mentioned above, the unidirectional anisotropy field induced by field cooling, if significant compared to disordering fields (random field, random anisotropy), causes the hysteresis loop to have a greater slope near the coercive field. This switchinglike behavior also increases the coercivity because a larger field will be required to initiate the large avalanches that lead to the switching of the magnetization.[53]

The monotonic decrease in H_c^{ZFC} with increasing temperature and its vanishing at $T < T_f$ indicate that the hysteretic behavior and exchange bias in $Mn_{0.25}Ti_{1.1}S_2$ are associated with the cluster-glass phase. The decrease in H_c^{ZFC} as the temperature rises is due to increased thermal fluctuations. Another factor may be that anisotropy strength tends to decrease with increasing temperature.

Finally, we comment on the unusually high coercivity in $Mn_{0.25}Ti_{1.1}S_2$ at low temperatures. A possible reason for this is the existence of excess Ti ions intercalated along with the Mn ions. Pure TiS_2 samples that we prepared exhibited paramagnetic behavior down to 2 K—our lowest accessible temperature. This paramagnetic behavior is likely due to intercalated Ti^{3+} ions. These ions are present in $Mn_{0.25}Ti_{1.1}S_2$ as well. The intercalated ions would enhance the probability of spin-orbit scattering between Mn^{2+} ions, leading to increased strength of the DM interaction. We note that the DM interaction has been strengthened in the $Cu_{1-x}Mn_x$ spin glass by the addition of Au or Pt impurities.[54]

V. CONCLUSIONS

We have performed magnetic measurements on the Mn-intercalated transition-metal dichalcogenide material $Mn_{0.25}Ti_{1+y}S_2$, which also had an excess intercalated Ti concentration $y \approx 0.1$. For temperatures between 100 and 300 K, $Mn_{0.25}Ti_{1.1}S_2$ exhibits Curie-Weiss paramagnetic behavior. The effective moment of a single Mn ion was found to be $\mu_{eff}=6.07\pm0.23$ μ_B; thus, the magnetism is due to local Mn^{2+} moments. A Curie-Weiss temperature $\Theta_{CW}=-26\pm1$ K indicated nearest-neighbor antiferromagnetic interactions. For $T<100$ K, deviation from Curie-Weiss behavior signified the onset of short-range AF order. The zero-field-cooled and field-cooled magnetizations bifurcated at $\sim$20 K; below this temperature, the system froze into a cluster-glass state. In the CG regime, the system exhibited hysteresis and exchange bias. The magnetization as a function of field at 2 K in the CG regime was fit with a two-component function: one was linear in the field; the other described the hysteretic behavior with a phenomenological function. The fitting parameters included the coercivity, saturation magnetization, and squareness of the hysteretic component of the magnetization. Our key findings were: (i) the ZFC coercivity was lower than the FC coercivity; (ii) for cooling field strengths between 20 and 50 kOe, the exchange-bias field decreased with increasing cooling field; (iii) the ZFC coercivity decreases with increasing temperature; and (iv) a relatively large ZFC coercivity for a system of Mn^{2+} moments that vanished at a temperature below the zero-field cluster-glass freezing temperature. The behavior of the system was explained in terms of a model based on antiferromagnetically correlated clusters with regions of uncompensated spins at the surfaces. The relatively large coercivity is likely attributable to an enhanced Dzyaloshinskii-Moriya interaction strength due to spin-orbit scattering by the intercalated excess Ti ions.

ACKNOWLEDGMENTS

The authors are grateful to M. McGarvey and S. Markova for their assistance with data analysis. This work was supported by NSF under Grant No. DMR 5040177, Iowa Office of Energy Independence under Award No. 09-IPF-11, and Battelle.

[1] R. H. Friend and A. D. Yoffe, Adv. Phys. **36**, 1 (1987).
[2] M. Inoue, H. P. Hughes, and A. D. Yoffe, Adv. Phys. **38**, 565 (1989).
[3] T. E. Kidd, T. Miller, M. Y. Chou, and T. C. Chiang, Phys. Rev. Lett. **88**, 226402 (2002).
[4] H. Cercellier, C. Monney, F. Clerc, C. Battaglia, L. Despont, M. G. Garnier, H. Beck, P. Aebi, L. Patthey, H. Berger, and L. Forró, Phys. Rev. Lett. **99**, 146403 (2007).
[5] C. Monney, H. Cercellier, C. Battaglia, E. F. Schwier, C. Didiot, M. G. Garnier, H. Beck, and P. Aebi, Physica B **404**, 3172 (2009).
[6] J. van Wezel, P. Nahai-Williamson, and S. S. Saxena, EPL **89**, 47004 (2010).
[7] E. Morosan, H. W. Zandbergen, B. S. Dennis, J. W. G. Bos, Y. Onose, T. Klimczuk, A. P. Ramirez, N. P. Ong, and R. J. Cava, Nat. Phys. **2**, 544 (2006).
[8] S. L. Bud'ko, P. C. Canfield, E. Morosan, R. J. Cava, and G. M. Schmiedeshoff, J. Phys.: Condens. Matter **19**, 176230 (2007).
[9] E. Morosan, L. Li, N. P. Ong, and R. J. Cava, Phys. Rev. B **75**, 104505 (2007).
[10] D. Qian, D. Hsieh, L. Wray, Y. Xia, R. Cava, E. Morosan, and M. Hasan, Physica B **403**, 1002 (2008).
[11] T. Yoshioka and Y. Tazuke, J. Phys. Soc. Jpn. **54**, 2088 (1985).
[12] H. Negishi, A. Shoube, H. Takahashi, Y. Ueda, M. Sasaki, and M. Inoue, J. Magn. Magn. Mater. **67**, 179 (1987).
[13] K. Binder and A. P. Young, Rev. Mod. Phys. **58**, 801 (1986).
[14] J. A. Mydosh, *Spin Glasses: An Experimental Introduction* (Taylor & Francis, Washington, DC, 1993).
[15] Y. Tazuke, S. Shibata, K. Nakamura, and H. Yano, J. Phys. Soc. Jpn. **64**, 242 (1995).
[16] R. M. A. Leith and J. C. J. M. Terhell, in *Preparation and Crystal Growth of Materials with Layered Structures*, edited by R. M. A. Leith (D. Reidel, Dordrecht, 1977), p. 162.
[17] Y. Tazuke, J. Magn. Magn. Mater. **140-144**, 155 (1995).
[18] J. S. Kouvel, J. Appl. Phys. **31**, S142 (1960).
[19] J. S. Kouvel, J. Phys. Chem. Solids **21**, 57 (1961).
[20] M. Inoue and H. Negishi, J. Phys. Chem. **90**, 235 (1986).
[21] M. Inoue, M. Koyano, H. Negishi, Y. Ueda, and H. Sato, Phys. Status Solidi B **132**, 295 (1985).
[22] N. Marcano, J. C. Gomez Sal, J. I. Espeso, L. Fernandez Barquin, and C. Paulsen, Phys. Rev. B **76**, 224419 (2007).
[23] S. Wakimoto, S. Ueki, Y. Endoh, and K. Yamada, Phys. Rev. B **62**, 3547 (2000).
[24] E. De Biasi, C. A. Ramos, R. D. Zysler, and H. Romero, Phys. Rev. B **65**, 144416 (2002).
[25] M. A. Morales, D. S. Williams, P. M. Shand, C. Stark, T. M. Pekarek, L. P. Yue, V. Petkov, and D. L. Leslie-Pelecky, Phys. Rev. B **70**, 184407 (2004).
[26] D. S. Williams, P. M. Shand, T. M. Pekarek, R. Skomski, V. Petkov, and D. L. Leslie-Pelecky, Phys. Rev. B **68**, 214404 (2003).
[27] A. Senchuk, H. P. Kunkel, R. M. Roshko, C. Viddal, L. Wei, G. Williams, and X. Z. Zhou, Eur. Phys. J. B **37**, 285 (2003).
[28] K. H. Fischer and J. A. Hertz, *Spin Glasses* (Cambridge University Press, Cambridge, 1991).
[29] S. N. Kaul and S. Srinath, J. Phys.: Condens. Matter **10**, 11067 (1998).
[30] J. R. L. de Almeida and D. J. Thouless, J. Phys. A **11**, 983 (1978).
[31] M. Gabay and G. Toulouse, Phys. Rev. Lett. **47**, 201 (1981).
[32] M. Gruyters, Phys. Rev. Lett. **95**, 077204 (2005).
[33] G. Kotliar and H. Sompolinsky, Phys. Rev. Lett. **53**, 1751 (1984).
[34] P. A. Joy, P. S. Kumar, and S. K. Date, J. Phys.: Condens. Matter **10**, 11049 (1998).
[35] M. Stearns and Y. Cheng, J. Appl. Phys. **75**, 6894 (1994).
[36] X. Liu, Y. Sasaki, and J. K. Furdyna, Appl. Phys. Lett. **79**, 2414 (2001).
[37] J. K. Furdyna, J. Appl. Phys. **64**, R29 (1988).
[38] A. Andreanov, J. T. Chalker, T. E. Saunders, and D. Sherrington, Phys. Rev. B **81**, 014406 (2010).
[39] J. S. Gardner, M. J. P. Gingras, and J. E. Greedan, Rev. Mod. Phys. **82**, 53 (2010).
[40] A. P. Ramirez, G. P. Espinosa, and A. S. Cooper, Phys. Rev. Lett. **64**, 2070 (1990).
[41] M. W. Roth, P. M. Shand, and T. E. Kidd (unpublished).
[42] M. Inoue, M. Matsumoto, H. Negishi, and H. Sakai, J. Magn. Magn. Mater. **53**, 131 (1985).
[43] M. Gruyters, EPL **77**, 57006 (2007).
[44] U. Nowak, K. D. Usadel, J. Keller, P. Miltenyi, B. Beschoten, and G. Guntherodt, Phys. Rev. B **66**, 014430 (2002).
[45] O. Iglesias, X. Batlle, and A. Labarta, J. Phys.: Condens. Matter **19**, 406232 (2007).
[46] R. H. Kodama and A. E. Berkowitz, Phys. Rev. B **59**, 6321 (1999).
[47] J. Nogués and I. K. Schuller, J. Magn. Magn. Mater. **192**, 203 (1999).
[48] M. Thakur, M. Patra, K. De, S. Majumdar, and S. Giri, J. Phys.: Condens. Matter **20**, 195215 (2008).
[49] D. Niebieskikwiat and M. B. Salamon, Phys. Rev. B **72**, 174422 (2005).
[50] J. Geshev, J. Magn. Magn. Mater. **320**, 600 (2008).
[51] G. Bertotti and M. Pasquale, J. Appl. Phys. **67**, 5255 (1990).
[52] F. Pázmándi, G. Zaránd, and G. T. Zimányi, Phys. Rev. Lett. **83**, 1034 (1999).
[53] J. P. Sethna, K. Dahmen, S. Kartha, J. A. Krumhansl, B. W. Roberts, and J. D. Shore, Phys. Rev. Lett. **70**, 3347 (1993).
[54] P. M. Levy and A. Fert, Phys. Rev. B **23**, 4667 (1981).